Population distributions in Li vapor excited by a photoionization electron source

R. G. Caro and J. C. Wang*

Edward L. Ginzton Laboratory, Stanford University, Stanford, California 94305
(Received 8 April 1985)

A detailed theoretical and experimental investigation is presented of the excited-level population distribution in a Li-Ne vapor under excitation by a photoionization electron source. This source produces a subnanosecond burst of hot $(T_e \sim 20$ eV) electrons with a peak density in excess of 5×10^{15} cm^{-3}. The electrons are generated as a result of photoionization of Ne atoms by x rays emitted from a plasma produced by a 100-mJ laser pulse of 600 ps duration. Measurements of Li($1s^2 2p$)-atom density, and of electron density, have been performed with subnanosecond time resolution under various conditions of excitation. A comprehensive rate-equation model is described and its predictions are seen to be in good agreement with experiment. It is shown that the population distribution in the Li-Ne vapor is strongly influenced by recombination. Under the conditions of these experiments, rates for this process as high as 3×10^9 s^{-1} were observed.

I. INTRODUCTION

Recently, Wang, Caro, and Harris[1] described a novel technique for generating high densities of hot photoelectrons. In order to produce these hot electrons, the soft x rays emitted from a laser-produced plasma were used to photoionize an "absorber" rare gas. Consequently, a subnanosecond burst of electrons was created with an average energy of 45 eV and a density in excess of 5×10^{15} cm^{-3}. This electron source was used to study the production, and subsequent deexcitation, of the metastable Li($1s\,2s\,2p$)$^4P^0$ level at 57.4 eV—a member of a class of atomic levels that is of interest because of the suitability of its elements as storage states for recent extreme ultraviolet (xuv) laser proposals.[2,3]

The photoionization electron source (PES) is uniquely suited to the excitation of highly energetic atomic levels (10–100 eV), because of the high temperature of the electrons that are produced. However, the large flux of hot electrons generated by the PES also results in very efficient excitation of less energetic lower atomic levels as well as of ionic species. In particular, it has been found that PES excitation is a very effective means by which to excite large densities of alkali-metal atoms to the first resonance level. For example, densities of Li($1s^2 2p$) atoms of 7×10^{16} cm^{-3} have been measured under conditions where the Li$^+$ ion density was only 2–3 % of the total initial density of Li atoms (10^{17} cm^{-3}).

Population distributions of this type, with high alkali-metal-atom resonance level density and low alkali-metal ion density, are of interest for a number of possible applications. Some examples of these are for the study of radiative collision lasers,[4] alkali-metal–rare-gas excimer lasers,[5–7] and xuv spectroscopy,[8,9] and for possible applications in nonlinear optics. In addition, any attempt to use the PES as an excitation source for an xuv laser[2,3] requires an understanding of the effect of the PES excitation on the population of the lower level of the potential xuv laser transition. In this paper we present a detailed investigation, both experimental and theoretical, of the

population distribution in an alkali-metal vapor, Li, that has been subjected to excitation by the PES.

An important aspect of the PES is its short temporal duration. Hot electrons are produced as a result of photoionization of an absorber gas—in this case Ne—by soft x rays emitted from a laser-produced plasma. In this work, the plasma was produced by a 1.06-μm laser with a pulse width of 600 ps. The x-ray emission is believed to have had a comparable duration.[10] Since the electrons lose energy by inelastic collisions on a time scale much shorter than this pulse width, the electron distribution was rapidly cooled after the termination of the laser pulse, and significant excitation by electrons ceased.

Because of the short time scale of the excitation produced by the PES, an investigation of the temporal development of the population distribution in the alkali-metal vapor involved population measurements with resolution on the subnanosecond time scale, as well as the theoretical analysis of processes with time constants of comparable magnitude. The experimental investigation described in Secs. II and III involved measurements of the Li($1s^2 2p$) population under various conditions of excitation and at various times after the initial PES excitation. In addition, measurements were made of electron density under two sets of excitation conditions. The results obtained from these measurements show that an extremely nonequilibrium distribution exists, both among the atomic levels in Li and with the Li$^+$ ion.

In essence, the nonequilibrium nature of the population distribution in the Li vapor following PES excitation is a result of the short duration of the excitation. However, the detailed time development of the alkali-metal-atom population distribution, subsequent to excitation by the PES, can only be understood by means of a rate-equation model such as is described in Sec. IV. In particular, in the course of the analysis it became apparent that recombination played a very important role in the development of the population distribution, even on the subnanosecond time scale. The demonstration of conditions under which such rapid recombination occurs may have important im-

plications for the development of recombination lasers.[11,12]

II. EXPERIMENTAL

A. PES excitation

The experimental configuration in which atomic vapor has been excited by means of the photoionization source has been described in detail elsewhere.[1,13,14] It is illustrated in Fig. 1. A massive plane tantalum target was placed inside a cell containing a mixture of the rare-gas absorber, Ne, and the target species, Li. A 60-mJ, 600-ps pulse from a Nd:YAG (yttrium aluminum garnet) laser (1.06 μm) was focused onto the target and a plasma was formed. For the focal spot intensity (10^{13} W cm^{-2}) and the pulse length used in this work, the resulting soft x-ray emission can be considered[14] as that of a blackbody with a temperature between 10 and 100 eV. The corresponding conversion efficiency from 1.06-μm radiation to x rays was estimated[14] to be in excess of 10%. The x rays emitted from the plasma propagated into the surrounding medium and photoionized the absorber Ne atoms to produce high densities of hot electrons.

B. Li($1s^2 2p$) population measurements

A major cooling mechanism for the photoelectrons produced by the PES is that of inelastic collisions with Li atoms, resulting in excitation of the Li($1s^2 2p$) level at 1.8 eV. It was thus desirable to be able to measure the population in this level in order to understand the behavior of the Li-Ne system under excitation by the PES. At frequencies around an atomic transition, the (complex) refractive index of the medium is dependent on the population in the upper and lower levels of the transition. Thus, knowledge of either the real or imaginary parts of the refractive index of the medium can provide information about the density of atoms in these levels. To measure the density of Li atoms excited by the PES to the Li($1s^2 2p$) level, either the absorption or refractive index (real) of the medium was examined in the vicinity of a suitable Li($1s^2 2p$-$1s^2 nl$) transition. To do this, a probe laser beam was passed through the region of vapor that was excited by the PES and was tuned through various transitions originating on the Li($1s^2 2p$) level. By adjusting the relative timing between the probe laser and the PES plasma-

FIG. 1. Schematic of experimental configuration.

producing laser, time-resolved measurements could be made of the Li($1s^2 2p$) population.

In order to examine the *absorption* of the probe beam as its frequency was tuned through the Li($1s^2 2p$-$1s^2 nl$) transition, a portion was split off and used as a reference beam. The energies in both the reference beam and the transmitted beam were recorded by photodiodes and the ratio of the two signals was taken electronically to minimize the effect of fluctuations in the probe beam intensity. After averaging over 1—10 shots, absorptions as small as 5% could be measured. By comparing the absorption traces with the theoretical predictions given by numerically generated Voigt profiles, a measurement of the product ($N^* fL\, \delta\omega_L$) could be obtained.[15] However, to deduce the value of the number density-length product, N^*L, of excited atoms, knowledge of the magnitude of the dominant Lorentzian component, $\delta\omega_L$, of the transition linewidth was required.

The linewidths of transitions, such as Li($1s^2 2p$-$1s^2 nd$), which were suitable for monitoring the Li($2p$) population had contributions from both pressure broadening and Stark broadening under the conditions of this experiment. Because of uncertainty in the values of the relevant broadening coefficients as well as of the electron density in the medium, the measurements of the product ($N^* fL\, \delta\omega_L$) could not be readily converted to accurate values of N^*L. An alternative to this "absorption" method of population measurement is to examine the *real* part of the refractive index, many linewidths from line center where its value is independent of the transition linewidth. Although population measurements made by examining the refractive index of the medium are less sensitive than those based on measurements of absorption, they have the important advantage that no knowledge is required of the transition linewidth to yield highly accurate values of the excited-state density-length product, N^*L.

To perform such a measurement, the probe beam was split into two beams of equal intensity which were then recombined at the output of a Mach-Zehnder interferometer. The cell was placed in one arm of the interferometer and the probe laser was tuned through the transition from the excited Li($1s^2 2p$) level while the output of the interferometer was monitored. This experimental geometry is illustrated in Fig. 2.

In order to minimize the effect of air currents, the entire interferometer was enclosed in a Plexiglas box. The relative path lengths in the two arms of the interferometer were adjusted by inserting silica blocks into the reference arm of the interferometer. Each arm of the interferometer was approximately 1 m long, and it was necessary to equalize the path lengths to better than 1 mm. Although the interferometer mirrors were simply mounted on a standard optical table, and the PES cell was kept at a temperature in excess of 900 °C and mounted on the table in one arm of the interferometer, no stability problems were observed for scan lengths of the order of 10 min. Long-term stability and reproducibility were also excellent.

The interferometer pattern at the exit of the Mach-Zehnder interferometer was projected onto a slit placed parallel to the straight fringes of the pattern. The slit
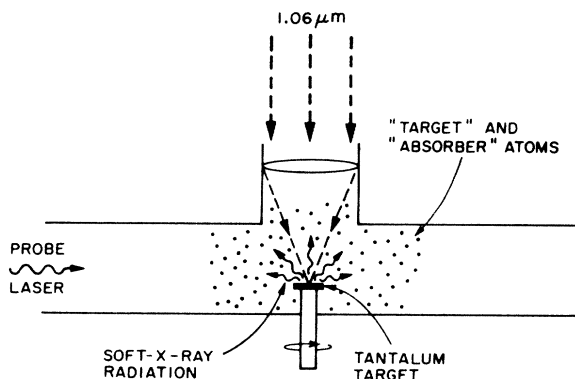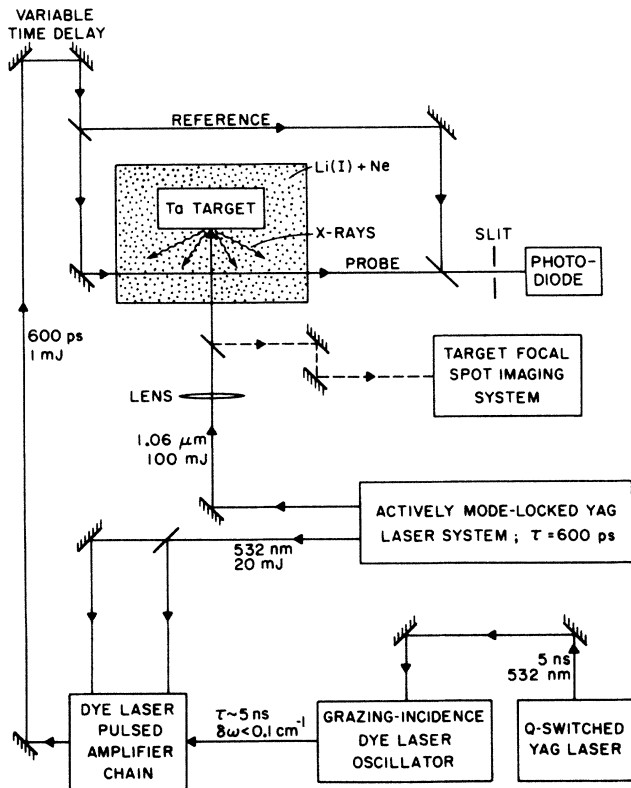
FIG. 2. Experimental system.

width was set at less than one fringe width. As the dye-laser wavelength was changed, the fringe maxima moved across the slit. A photodiode, positioned to monitor the light transmitted through the slit, detected an oscillating intensity as the dye laser was tuned. The scan rate of the laser wavelength was monitored by recording the transmission of a Fabry-Perot etalon. An example of the interferometer signal is shown in Fig. 3.

INTERFEROMETER FRINGE SCAN
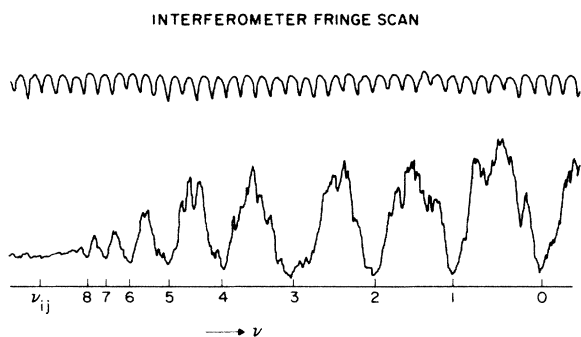
FIG. 3. Lower trace: the Mach-Zehnder interferometer output as the probe laser was tuned through the $Li(1s^2 2p\text{-}1s^2 3d)$ transition at v_{ij}. Upper trace: the Fabry-Perot etalon output (FSR is 3.4 cm^{-1}) used as wave-number calibration. Li density is 10^{17} cm^{-3}, Ne density is 0 cm^{-3}, distance from target is 1 mm, time after peak of plasma-producing laser pulse is 1.2 ns.

III. ANALYSIS AND RESULTS

Conceptually, the interferometric method used in this work to measure the $Li(1s^2 2p)$ population is analogous to the well-known hook method, first developed by Rozhdestvenskii[16] and reviewed by Marlow.[17] An important modification of this method has been described by Duval and McIntosh[18] and it is that technique which has been used here. In the original demonstration of their interferometric measurement, Duval and McIntosh[18] were able to accurately measure the oscillator strength of the Cs(6s-7p) transition. The measurements described here represent the first reported demonstration of one of the most significant features of the Duval-McIntosh technique—namely, its suitability for the accurate measurement of excited-state populations with subnanosecond time resolution.

Following Duval and McIntosh,[18] the phase difference Φ between the two beams in the Mach-Zehnder interferometer can be written as

$$\Phi = 2\pi v[D + (n-1)L] , \qquad (1)$$

where $v = 1/\lambda$ is the wave number of the illuminating beam, n and L are the refractive index and length of the cell, and $D = d - (n_0 - 1)L$, where d is the geometric difference in path length of the two arms of the interferometer and n_0 is the refractive index in the reference arm.

In the neighborhood of a single spectral line, the refractive index in the vapor excited by the PES is given by the Sellmeier equation:

$$n - 1 = \beta N_i f_{ij} / [v_{ij}(v_{ij} - v)] , \qquad (2)$$

where N_i, f_{ij}, and v_{ij} are, respectively, the population in the lower level of the transition and the oscillator strength and wave number of the transition from level i to j, and $\beta = e^2 / 16\pi^2 \epsilon_0 mc^2$. Using Eqs. (1) and (2) it can be shown that the fringe number k occurs at a wave number v_k given by

$$Dv_k + S/(v_{ij} - v_k) = k , \qquad (3)$$

where $S = \beta N_i f_{ij} L$. As can be seen in Fig. 3, far from the transition v_{ij} (in this case $Li[(1s^2 2p)\text{-}(1s^2 3d)]$), the fringe spacing is regular and determined only by D (and thus by the path length between the interferometer arms). As $v \rightarrow v_{ij}$, the fringes get closer and closer. Also, the effect of absorption in the cell decreases the fringe contrast.

By recording the relative position and number of the fringes, a least-squares fit can be made to Eq. (3) to obtain the values of D, S, and $v_{ij} - v_{(k=0)}$. The numbering of the fringes, k, can be relative to any arbitrary fringe position. In Fig. 4 is shown the position v_k of the fringes of the interferometer scan of Fig. 3 as a function of k. The solid line is a least-squares fit of Eq. (3) to the data. It can be seen that the fit is excellent. From the value of S that is provided by the least-squares-fitting procedure, a value of $N^* L = 2.5 \times 10^{15}$ can be deduced for the population density-length product of the $Li(1s^2 2p)$ population. The associated error is ±20%.

Using this interferometric measurement technique, $Li(1s^2 2p)$ population measurements have been made for
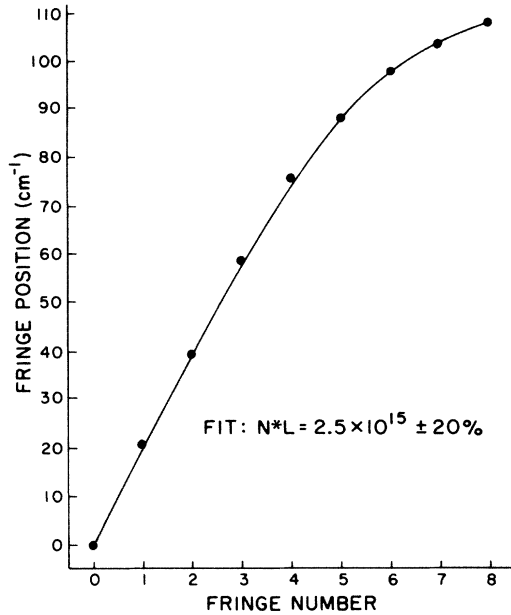
FIG. 4. Interferometer output fringe position dependence on fringe number for the scan of Fig. 3. The solid line is a least-squares fit to the Sellmeier equation which yields the result $N^*L = 2.5 \times 10^{15} \pm 20\%$ for the number density-length product of $Li(1s^22p)$ population.

TABLE I. $Li(1s^22p)$ number density (cm^{-3}) under conditions of various densities of neon and distances from the target. The probe laser was delayed by 1.2 ns with respect to the plasma-producing laser. The initial Li density was 10^{17} cm^{-3}.

Neon density $(10^{17}$ $cm^{-3})$	Distance from target (mm)		
	1	3	7.5
0	2×10^{16}	3×10^{15}	4×10^{14}
3	7×10^{16}	9×10^{15}	1×10^{15}
10	4×10^{16}	1×10^{16}	5×10^{14}

better than a factor of 2 in all cases and generally to be such as to have an error of less than $\pm 50\%$. The relationship between N^* and N^*L is dependent on the spatial x-ray radiation pattern assumed from the plasma. In particular, if an isotropic distribution is assumed rather than the conical one preferred by Caro et al.,[14] Eq. (4) yields values of N^* that are high by a factor of 2. In light of the theoretical results of Sec. IV, it seems quite possible that the values of Table I should be reduced by a factor of between 1 and 2 to allow for this.

In Fig. 5(a) is shown the dependence of $Li(1s^22p)$ population on the time delay between the probe laser and the "firing" of the PES by the plasma-producing laser. Also shown are various theoretical predictions that will be discussed further in Sec. IV. It can be seen from the measurements that a large fraction of the Li ground-state atoms are excited to the $Li(1s^22p)$ level and remain there for at least several nanoseconds.

different Ne densities, at a number of distances from the target and at various time delays after the plasma-producing laser pulse was incident on the target. In all cases, the initial Li density was 10^{17} cm^{-3}. Under such conditions, the mean free path of the PES electrons was very small and the spatial distribution of excited states should have been dependent only on the spatial distribution of the x rays propagating out from the target. As discussed by Caro et al.,[14] it seems reasonable to use the relationship

$$N^* = 2(N^*L)/\pi R \qquad (4)$$

to relate the excited-state density N^* (at a distance R along a path normal to the target) to the integrated excited-state density-length product N^*L along a probe beam at a distance R from, but in a plane parallel to that of, the target. Although the measurements that were made in this work were actually of N^*L, the values reported in this work for the $Li(1s^22p)$ density are of N^*. Equation (4) has been used to relate these two quantities.

A. $Li(1s^22p)$ measurements

Table I summarizes the dependence of $Li(1s^22p)$ population on Ne density and on distance from the target. All of these results were measured under conditions of initial Li-atom density of 10^{17} cm^{-3} and with time delays of approximately 1.2 ns between the arrival in the cell of the plasma-producing laser and the probe laser beams. The accuracy of the N^*L measurements is believed to be

B. Electron density measurement

In addition to the $Li(1s^22p)$ measurements, the electron density in the PES-excited Li vapor has been measured. As discussed in Sec. II, absorption measurements of excited-state populations yield values for the product $(N^*fL\ \delta\omega_L)$. Since the interferometric Duval-McIntosh technique yields values of N^*fL, a comparison of the results of these two techniques can lead to a value of $\delta\omega_L$. By choosing the $Li(1s^22p\text{-}1s^24d)$ transition at 460 nm, for which the dominant contribution to the Lorentzian linewidth, $\delta\omega_L$, is Stark broadening, a value of electron density can be deduced using the Stark-broadening coefficients reported by Griem.[19]

Measurements were made at 1 mm from the target at a time of 1.2 ns after the plasma-producing laser pulse and at a Li pressure of 10^{17} cm^{-3}. In the absence of Ne in the cell, a Lorentzian width of 2.6 cm^{-1} was deduced from the absorption measurements on the $Li(1s^22p\text{-}1s^24d)$ transition. For a density of 3×10^{17} cm^{-3} Ne atoms, the corresponding transition width was 2.9 cm^{-1}. Using the Stark-broadening coefficient of Griem[19] of 5.1 $\mathring{A}$ at an electron density of 10^{16} cm^{-3}, and taking into account a linewidth contribution[20] due to pressure broadening of 0.3 cm^{-1}, values of electron density can be deduced to be $N_e = (1.2\pm0.6) \times 10^{15}$ cm^{-3} in the absence of Ne and $N_e = (1.3\pm0.8) \times 10^{15}$ cm^{-3} in the presence of 3×10^{17} cm^{-3} Ne atoms.

At first glance this relatively low degree of ionization is surprising in light of the large "temperature" of the neutral Li levels. Also, the fact that there is little difference in the measured values of electron density between conditions of no Ne and of 3×10^{17} cm^{-3} Ne atoms in the cell seems inconsistent with the picture of Ne atoms acting as absorber atoms and providing electrons for the PES. Certainly, in the work of Wang, Caro, and Harris,[1] although copious excitation of the high-lying (60-eV) Li$(1s2s2p)^4P^0$

(a)

(b)

FIG. 5. Model predictions of the time dependence of population in the Li$(1s^22s)$, Li$(1s^22p)$, and Li$^+(1s^2)$ levels, of cold and hot electron density, and of cold electron temperature. The initial density of Li was 10^{17} cm^{-3} and that of Ne was 3×10^{17} cm^{-3}. The predictions are for a distance of 1 mm from the target. The peak of the plasma-producing laser is at time $t = 0.6$ ns. Experimental points are shown in (a) for the Li$(1s^22p)$ population and in (b) for the (total) electron density.

level was observed in the presence of Ne, this level was not observed to be excited when Ne was removed from the cell. As can be seen from Sec. IV, both of these apparent contradictions can be understood when the PES-excited Li-Ne system is modeled carefully.

IV. THEORETICAL ANALYSIS; RATE-EQUATION MODEL

To model the excitation of Li and Ne atoms and ions in the plasma formed by the PES, the first step is to examine the production of electrons by photoionization of Ne and Li atoms by the x rays emitted from the laser-produced plasma. These electrons are responsible for the excitation of the surrounding atoms and ions. The processes that have been determined to be important in modeling the PES are x-ray photoionization, electron ionization, electron inelastic collisions leading to atomic excitation and deexcitation (superelastic collisions), three-body collisional recombination, and electron-electron elastic collisions leading to thermalization of the electron bath.

A. Photoionization

As described elsewhere,[14] the x rays emitted from the laser-produced plasma can be considered as emanating from a blackbody with a characteristic temperature. For this model, best agreement with experiment was obtained using a temperature of 30 eV and a conversion efficiency from 1.06-μm photons to soft x rays of 10% (corresponding to an emitted soft x-ray energy of 6 mJ). The radiation was modeled as being emitted into a cone with a 45° half-angle and an axis normal to the target.

The intensity of soft x rays, $I(\omega)$, per unit bandwidth at frequency ω, at a distance R from, and along a normal to, the target, can thus be written as $I(\omega) = f(t)B(\omega)$. Here $B(\omega)$ is the soft x-ray intensity integrated over the x-ray pulse duration:

$$B(\omega) = \frac{A \tau \hbar \omega^3 \exp[-\alpha(\omega)R]}{8\pi^3 c^2 qR^2[\exp(\hbar\omega/kT)-1]} , \qquad (5)$$

where $\alpha(\omega)$ is the absorption coefficient of the vapor, τ is the duration of the pulse, and q is a coefficient which determines the radiation pattern of the x rays ($q = 0.3$ for conical emission, $q = 1$ for isotropic emission). T is the temperature of the blackbody, and A is the effective surface area of the blackbody. Under the model conditions of 6 mJ of emitted soft x-ray energy and a temperature of 30 eV, the blackbody surface area would be equivalent to that of a disc with a radius of 120 μm. The 1.06-μm laser beam is focused to a spot size of approximately 30–100 μm and so such blackbody dimensions seem reasonable.

The function $f(t)$ is a weighting function to take into account the temporal shape of the x-ray emission, which is assumed to have a similar temporal dependence to that of the 1.06-μm laser pulse.[10] In this work, $f(t)$ is considered to be of a triangular shape with a half-width of 600 ps. Thus, at a time t, the probability for photoionization of an atom of species A to occur is given by

$$W_I^A = \int [\sigma_I^A(\omega)I(\omega)/\hbar\omega]d\omega , \qquad (6)$$

where $\sigma_I^A(\omega)$ is the cross section for photoionization of atom A.

In a time interval Δt, the ejected electrons produced by x-ray photoionization of atoms A and B can be described by the distribution $[\bar{n}(E)f(t)\Delta t]$, where

$$\bar{n}(E) = \frac{N_A\sigma_I^A(\omega_1)B(\omega_1)}{\hbar\omega_1} + \frac{N_B\sigma_I^B(\omega_2)B(\omega_2)}{\hbar\omega_2} , \qquad (7)$$

where $E = \hbar\omega_1 - E_I^A = \hbar\omega_2 - E_I^B$, and E_I^N is the ionization energy of atom N. In the absence of collisions to alter the energy distribution of the electrons, the electron distribution at the end of the x-ray emission pulse would be given by $\bar{n}(E)$. A typical example of such a distribution is shown in Fig. 6 for photoionization of the absorber gas Ne. The distribution $\bar{n}(E)$ is characterized by a total electron density $N_e = \int \bar{n}(E)dE$ and an average electron energy $\bar{E} = \int \bar{n}(E)E \, dE/N_e$.

Since electron collision times, under the conditions of the PES, are of the order of 10 ps—compared to an x-ray pulse width of 600 ps—the distribution $\bar{n}(E)$ is never actually realized. The real electron distribution in the PES cell has been modeled in the following ways. The most exact method is to recalculate the complete electron distribution $n(E)$ after each time interval Δt, taking into account electron production by photoionization and electron ionization, as well as electron cooling and heating by collisions and electron loss by recombination. An alternative
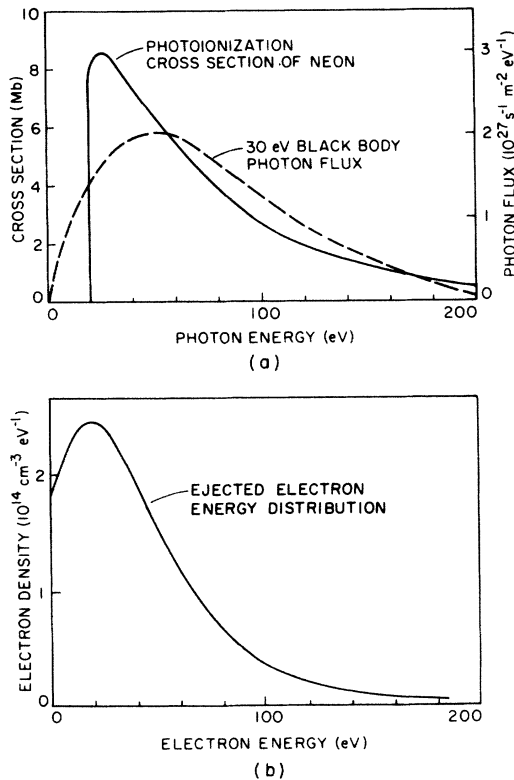
method, involving less computation, is to consider the electrons in the PES plasma to be divided into two classes: a "hot" class and a "cold" class. The cold electron distribution is considered to be a Boltzmann distribution, characterized by a temperature T_e (typically < 1 eV). The hot electron class is considered to be a monoenergetic ensemble of electrons with energy $\bar{E}/2$. This latter approach has been shown to yield comparable results to the more exact method above, and it is this two-component electron distribution which has been used in the work described in this paper.

In a time interval Δt, hot electrons are produced by photoionization at a rate of $\partial n_H/\partial t = N_e f(t)$. A cooling rate for these electrons, due to inelastic collisions with atoms or ions, is of the form $Q = N\sigma v_e E$, where N is the atom density, σ and E are the cross section and energy loss applicable to the dominant collision process, and v_e is the electron velocity. Then hot electrons are passed to the cold electron class at a rate of $\partial n_H/\partial t = -n_H(t)Q/\bar{E}$, where $n_H(t)$ is the hot electron density.

Although both hot and cold electrons can cause ionization and can experience inelastic collisions, recombination affects only the cold electron class. Similarly, the electrons produced by the process of electron ionization are assumed to be created with an energy E_{cold} characteristic of the cold electron class. Since a typical time for thermalization of the cold electron class by electron-electron collisions is several picoseconds[21] (fast compared to cold electron production), the imposition of a Boltzmann distribution on the cold electron class seems justified.

B. Inelastic electron collisions

Cross sections for inelastic collisions of hot electrons with atoms can be calculated using the Bethe approximation.[22] In that approximation, the cross section for electron excitation (or deexcitation) from level i to level j is given by

$$\sigma_{ij}^H = e^4 f_{ij}\bar{g}/(4\sqrt{3}m\epsilon_0^2 v_e^2 \, |E_j - E_i|) . \qquad (8)$$

Here f_{ij} is the oscillator strength for the transition between the levels with energies E_i and E_j, m and v_e are the mass and velocity of the incident electron, and $\bar{g}$ is the Gaunt factor. For the purposes of this model, the Gaunt factor tabulated by van Regemorter[22] was used. Values of $\bar{g}$ were obtained empirically from experimental data and tabulated as a function of $x = (E/|E_i - E_j|)^{1/2}$, where E is the exit electron energy for excitation and the incident electron energy for deexcitation. When the Gaunt factor of van Regemorter is used, the formula of Eq. (8) is applicable to inelastic collisions with both hot and cold electrons.

When the cross section of Eq. (8) is averaged over the Boltzmann energy distribution of the cold electron class, an inelastic collision transition probability due to that class can be obtained. Following van Regemorter,[22] and using the approximation to the Gaunt factor $\bar{g}(x) \sim 0.0515x + 0.0725x^2$, we derive the approximate formula for deexcitation of level j to level i:

FIG. 6. Photoelectron energy distribution $\bar{n}(E)$ due to a neon density of 3×10^{17} cm^{-3} and a Li density of 10^{17} cm^{-3} at a distance of 1 mm from the target. The total electron density is 2×10^{16} cm^{-3}.

$$\langle \sigma_{ji}^c v_e \rangle = \left[\frac{2}{3\pi m k T_e} \right]^{1/2} \frac{e^4 f_{ij}}{4\epsilon_0^2 E_{ij}}$$

$$\times [(4.56 \times 10^{-2})y^{-1/2} + (7.25 \times 10^{-2})y^{-1}] \; , \tag{9}$$

where $y = E_{ij}/kT_e$, $E_{ij} = |E_i - E_j|$, and T_e is the cold electron distribution temperature. By the principal of detailed balance

$$\langle \sigma_{ij}^c v \rangle = \langle \sigma_{ji}^c v \rangle \exp(-E_{ij}/kT_e)g_j/g_i \; . \tag{10}$$

Expression (9) is a reasonable approximation as long as $y > 0.1$. For smaller values of y it seriously overestimates the collision cross sections; however, that regime is not applicable to this work.

C. Ionization

Electron ionization can be described classically in the manner discussed by Gryzinski.[23] For the hot electron class, we can write the cross section for ionization by an electron of energy E as

$$\sigma_I^H(E) = (\sigma_0/E_I^2)g_i(x)\xi_i \; , \tag{11}$$

where

$$g_i(x) = \frac{1}{x} \left[\frac{x-1}{x+1} \right]^{3/2}$$

$$\times \left[1 + \frac{2}{3} \left[1 - \frac{1}{2x} \right] \ln[2.7 + (x-1)^{1/2}] \right] \tag{12}$$

and $x = E/E_I$. E_I is the ionization energy of the atomic level from which ionization is to occur, ξ_i is the number of equivalent electrons in the shell whose ionization is being calculated, and $\sigma_0 = e^4/16\pi\epsilon_0^2$.

In the same way as for the process of electron excitation, this cross section can be averaged over the cold electron velocity distribution. That procedure is somewhat simplified by following the approach of Drawin and Emard[24] which yields the result

$$\langle \sigma_I^c v_e \rangle = 8\pi a_0^2 \left[\frac{E_H}{E_I} \right]^2 f_i \xi_i \left[\frac{2kT_e}{\pi m} \right]^{1/2} u_i \Psi(u_i) \tag{13}$$

with

$$\Psi(u) = \frac{\exp(-u)}{1+u} \left\{ \ln \left[1.25 \left[1 + \frac{1}{u} \right] \right] + \frac{1}{u+20} \right\} \; , \tag{14}$$

where $u_i = E_I/kT_e$, a_0 and E_H are the Bohr radius and binding energy of the hydrogen atom, and f_i is the oscillator strength for bound-free transitions.

D. Recombination

The only recombination process considered to be important in this work is the three-body collision

$$A^+ + 2e^- \rightarrow A^* + e^- \; . \tag{15}$$

Since the Rydberg levels of the light alkali-metal atoms are quite well described by hydrogenic wave functions, this recombination process can be relatively simply modeled.[25] The recombination rate from an ion A^+ with a degeneracy of g_+ to the level n of atom A is given by[25]

$$\alpha_n = \frac{64\pi^2 a_0^2 E_H \hbar^3 n^4 n_e}{m^2 g_+ (kT_e)^2} \; , \tag{16}$$

where E_H is the binding energy of hydrogen and n_e is the (cold) electron density. Alternatively, the total depletion rate of electrons due to three-body collisional recombination to atom A is given by[25]

$$\alpha_{tot} = \frac{64\pi^2 a_0^2 \hbar^3 n_e E_H^{7/2}}{5m^2 g_+ (kT_e)^{9/2}} \; . \tag{17}$$

Hence we can write the rate equations for recombination as

$$\frac{\partial N_+}{\partial t} = -N_+ n_e \alpha_{tot} \; , \tag{18a}$$

$$\frac{\partial N_n}{\partial t} = N_+ n_e \alpha_n \; , \tag{18b}$$

where N_n and N_+ are the populations, respectively, in level n of the atom and in the ion.

E. Model details

The PES plasma consisted of a two-component mixture of Li and Ne. The model considered the Li levels $1s^2 2s$, $1s^2 2p$, $1s^2(n = 3)$, and $1s^2(n = 4)$ discretely. It took account of the higher Li levels up to the $Li^+(1s^2)$ continuum in the form of a sum of hydrogenic Rydberg levels up to level n^*, where n^* was determined by the energy ΔE, by which the continuum was depressed due to the presence of free electrons. The value of ΔE was given by the Unsöld equation:[26]

$$\Delta E \sim \frac{3e^2}{4\pi\epsilon_0} \left[\frac{4\pi n_e}{3} \right]^{1/3} \; . \tag{19}$$

Hence one obtains the value $n^* = (R_{Li}/\Delta E)^{1/2}$, where R_{Li} is the Rydberg constant for Li.

Recombination and ionization from the discrete levels and the Rydberg series were included in the model, as was inner-shell electron ionization. Inelastic collisions with electrons causing transitions among the discrete levels—a major source of electron cooling—was explicitly included. However, cooling (or heating) due to inelastic electron-atom collisions with Rydberg-level Li atoms was included approximately only. These processes were modeled by including an electron cooling (heating) rate of 100 eV/ns for every 10^{16} cm^{-3} Li* atoms in the Rydberg levels. The energy gap associated with this cooling rate was taken to be 0.25 eV. From estimates of typical cooling rates by Rydberg levels in Li, this seems a reasonable "average" cooling rate. For comparison, cooling of hot electrons by inelastic collisions with Li ground-state atoms had a rate of 150 eV/ns at a Li density of 10^{17} cm^{-3}, while ionization

of Li at the same density cooled electrons at a rate of 120 eV/ns.

In Ne, the levels considered were the atomic ground state, the ion ground state, and a series of levels corresponding to neutral Rydberg levels. Inner- and outer-shell electron ionization and recombination were specifically included. The cooling rate for hot electrons, as a result of ionization of Ne at a density of 10^{17} cm^{-3}, was 45 eV/ns. Cooling due to the Ne Rydberg levels could be included in the same manner as for the Li Rydberg levels and at the same rate. Heating of the cold electron class by the three-body recombination process was included in the model directly. For Li, recombination and ionization between the continuum and the discrete levels were considered individually. However, in Ne only the "total" recombination rate [Eq. (17)] was used. It was possible to include in the model, empirically, supplemental electron cooling due to some unspecified process—for example, collisions with Li_2 or Li-Ne molecules.

Photoionization of both inner and outer shells of Li and Ne was considered. It was found to be unnecessary to include photoionization from higher levels of the atomic species or from the ionic species to the doubly charged ions. Photoexcitation to autoionizing levels[27] of Li was specifically included in the model and resulted in an increase in $Li^+(1s^2)$ population under some conditions. Electron excitation to autoionizing levels was not a significant process.

The rate-equation model described here consisted of a variable step-size computer program designed to solve multiple simultaneous atomic and ionic rate equations. Excitation rates were recalculated at each step. Maximum step sizes of 1 ps could be used but, under some conditions, steps of less than 10^{-15} s were required to maintain accuracy. The program was sufficiently simple to be run on a Hewlett-Packard HP-9836 microcomputer.

V. THEORETICAL RESULTS: COMPARISON WITH EXPERIMENT

In Figs. 5(a) and 5(b) are shown the predictions of the model for the time-varying populations in various species, together with the measured time dependence of the $Li(1s^22p)$ population, and one measurement of electron density. Two sets of model predictions are illustrated, with the difference between the two being the way in which inelastic collisions of electrons with Ne Rydberg atoms are treated. The predictions labeled as "no extra cooling" in Fig. 5 are for the case in which such collisions are ignored. The cold electron temperature is of the order of 0.6—0.7 eV under these conditions, and recombination, which has a $(T_e)^{-9/2}$ dependence [Eq. (17)], is not significant on the time scales under discussion. Because of this, the model predicts a much larger electron density and a much smaller $Li(1s^22p)$ population than were experimentally observed.

The population of excited Ne Rydberg atoms can be shown to be produced predominantly through recombination. Because this process preferentially fills the higher Ne levels, inelastic collisions with cool electrons will initially heat the electrons. Such heating would produce even poorer agreement between theory and experiment.

Simple thermodynamic arguments of this type are inappropriate here, however, because of the nonequilibrium nature of the plasma. Neon levels recombining to high levels do indeed initially give up energy to the cool electron class. However, there is a bottleneck at the $Ne(2p^53s)$ levels, 17 eV above the Ne ground state, where electron deexcitation occurs with a much longer time scale than is under consideration in this work. The dominant decay from these Ne levels is by radiative transitions to the ground state with time constants of the order of 1—10 ns, and two of the four levels in this configuration are metastable.

It is our hypothesis that, as a result of this bottleneck, the distribution of Ne atoms in the Rydberg levels acts to cool the electrons, for time scales of a few tens. of nanoseconds, once the $Ne(2p^53s)$ population has built up (10—100 ps). Such a cooling process has been included approximately in the model by assigning a cooling rate of 100 eV/ns for every 10^{16} cm^{-3} Ne* atoms in the Rydberg levels, as was done for excited Li atoms in similar levels. The predictions of the model including this cooling are labeled in Fig. 5 as "with extra cooling" and show reasonable agreement with experiment. All of the subsequent predictions of the model in this work include this source of electron cooling.

The best match to the measured $Li(1s^22p)$ populations of Table I was obtained by including in the model supplemental cooling at a rate of 10 eV/ns. This amount of extra cooling could be supplied by one, or several, of the processes that are not explicitly included in the model, for example, electron-Li_2 collisions. In Fig. 7 the populations in the $Li(1s^22p)$ level predicted by the model are shown together with the measured values from Table I. The agreement of the experimental data with the model predictions is reasonable. The predictions shown in Fig. 7 are for populations at a time 1.2 ns after the peak of the laser pulse—corresponding to the conditions of the experiment.

Also illustrated in Fig. 7 is the effect of eliminating the recombination process [Eq. (15)] from the model. Clearly, this process is very important—even on the subnanosecond time scales involved here. A further example of this is shown in Fig. 8 where the model predictions of electron density at $t = 1.2$ ns are shown together with the two data points measured experimentally. For all the model results illustrated in Fig. 8, the prediction of cold electron temperature is approximately 0.1 eV. The extremely rapid recombination seen here is due to the low temperature and relatively large electron density present in the PES plasma. The recombination rate of Eq. (17) depends on $n_e(kT_e)^{-9/2}$ and is thus a strong function of these parameters.

It should be noted that inclusion of the supplemental cooling rate of 10 eV/ns in the model has only a small effect on the model predictions. At 1 and 7.5 mm it has a negligible effect, but at 3 mm it serves to decrease electron density and temperature by a factor of 2—5. Although the larger values obtained by eliminating this extra cooling are not unreasonable, it seems likely that some such source of cooling exists due to molecules. Increasing the supplemental cooling rate has very little effect on any of
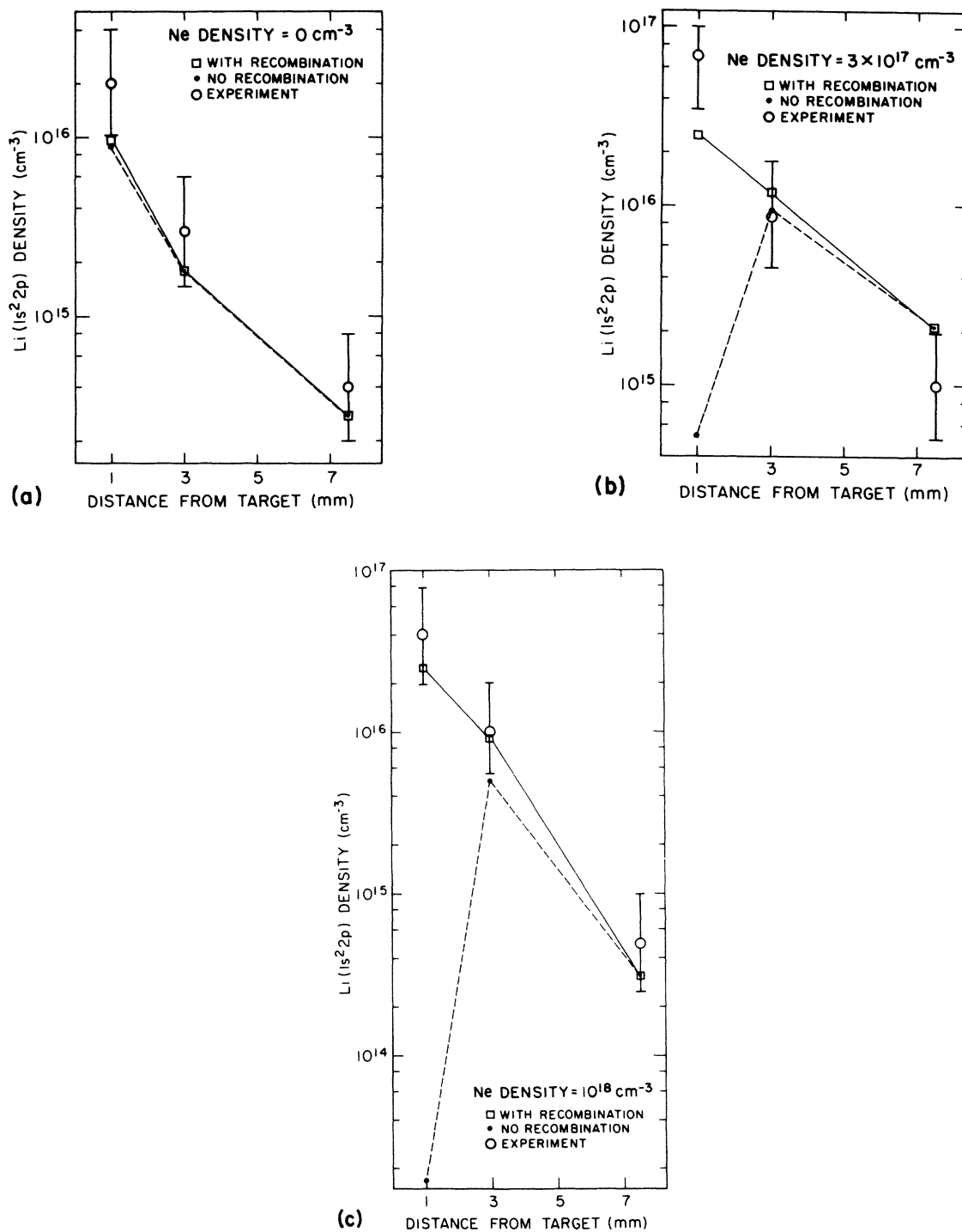
FIG. 7. Li($1s^2 2p$) density as a function of distance from the target. Experimental measurements and model predictions are shown for three Ne densities. The data are for an initial Li density of 10^{17} cm^{-3} and at a time 1.2 ns after the peak of the plasma-producing laser pulse.

the model predictions.

The conditions of the model were chosen to give the best fit to the experimental data for excitation by the PES of 10^{17} cm^{-3} Li atoms and 3×10^{17} cm^{-3} Ne atoms. The agreement with the experimental results is generally better than a factor of 2—comparable with the experimental er-

ror. It should be noted that the model predictions are not very sensitive to the temperature assumed for the x-ray-emitting blackbody, but are strongly dependent on the total number of electrons produced by photoionization during the course of the PES pulse.
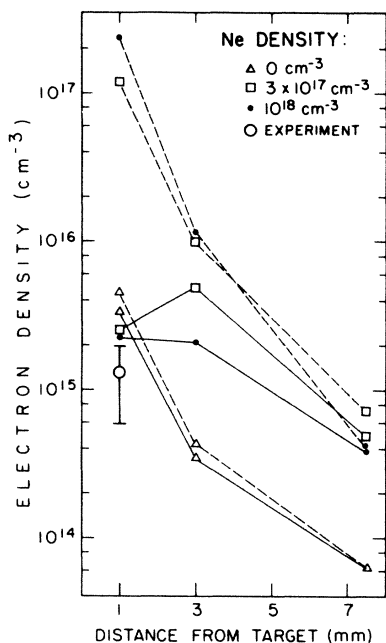
FIG. 8. Cold electron density vs distance from the target. The experimental data point represents the conditions of both 0 cm^{-3} Ne density and 3×10^{17} cm^{-3} Ne density. The model predictions are shown for three Ne densities. The solid lines represent the predictions of the model including recombination; the dashed lines show the predictions without recombination. The data presented are for an initial Li density of 10^{17} cm^{-3} and at a time 1.2 ns after the peak of the plasma-producing laser pulse.

VI. DISCUSSION

It is interesting to note the somewhat counterintuitive conditions that prevail in the PES-excited plasma. The cold electron class has a temperature of the order of 0.1 eV while the Li atoms have a very high "temperature" as evidenced by the large Li($1s^2 2p$) population. At the same time, the temperature of the cool electron class is only just beginning to rise at the end of the 10-ns period under examination. Such conditions are possible in a plasma that is far from thermodynamic equilibrium, as is this one. The temperature of the Li atoms is defined by the interaction with the class of hot electrons with a temperature on the order of 15 eV. The class of cool electrons continues to cool due to collisions with the Li atoms and the large bath of neutral Ne atoms—including the excited Ne atoms in the Ne($2p^5 3s$) levels. Although the cool electron temperature is low, the *total* electron temperature is given by a weighted average of the temperatures of both electron classes and is thus rather higher. Given a long enough time interval for equilibrium to be reached, all electrons will be found in the cool electron class, the temperature of which will define the population distributions of the atomic systems in the PES-excited plasma.

The most striking aspect of the modeling of the PES

excitation of the Li-Ne mixture is the rapid cooling of electrons and the subsequent subnanosecond recombination rates which hold the electron density in the PES at around 10^{15} cm^{-3}. At the same time, the presence of the hot electron class leads to very rapid electron excitation rates of energetic atomic transitions. The rapid recombination process appears to be a relatively general effect associated with PES excitation under conditions of high x-ray fluxes, such as were present in this work at a distance of 1 mm from the target. It can be seen from Figs. 7 and 8, however, that the importance of the recombination process is greatly reduced at larger distances from the target (or lower x-ray fluxes).

Similar rapid recombination has been observed by the authors—by monitoring the linewidths of Stark-broadened lines—during PES excitation of Na and also of He. In both cases, very efficient inner-shell excitation was observed [to, respectively, the Na($1s^2 2p^5 3s 3p$)$^4 D_{7/2}$ and Na$^+$($1s^2 2p^5 3s$)$^3 P_2$ levels, and the He($1s 2s$)$^1 S$ level], although rapid recombination kept the electron density low. In the case of the Na $^4 D_{7/2}$ excitation, the linewidth of the Na[($2p^5 3s 3p$)$^4 D_{7/2}$-($2p^5 3s 3d$)$^4 F_{9/2}$] transition, for which Stark broadening provided the dominant contribution, could be observed to decrease rapidly with time. This was a striking illustration of the rapid electron recombination predicted by our model. Our observations correspond to a decrease of electron density, by a factor of 5—10, to a final value of approximately 2×10^{15} cm^{-3} after a 4-ns interval.

Rapid recombination has been observed in this work, both directly in the case of the excitation of Na($1s^2 2p^5 3s 3p$) atoms and indirectly in the case of the Li excitation discussed earlier. In the case of Li, this rapid recombination is inferred because of the low electron density (10^{15} cm^{-3}) measured in the PES-excited mixture of Li and Ne at 1.2 ns after the peak of the plasma-producing laser pulse. Implicit in this inference is the belief that high electron densities are present earlier in time. This belief is completely supported by both the high Li($1s^2 2p$) populations and the large Li($1s 2s 2p$) populations that have been measured.[1]

This rapid recombination can be well explained by the model described here, providing the electrons in the cold electron class are sufficiently cool. Due to inelastic collisions with Li($1s^2 2s$), Li($1s^2 2p$), and Ne($1s^2 2s^2 2p^6$) atoms, the cold electron class can be shown to cool to 0.6—0.7 eV [Fig. 5(b)]. We hypothesize that bottlenecking in the Ne($2p^5 3s$) level provides an extra supply of atoms which act to cool the electrons by inelastic collisions. This extra cooling of electrons would produce temperatures in the cold electron class that would result in rapid recombination consistent with experimental observations.

The occurrence of this buildup of population in the Ne($2p^5 3s$) level, and the resultant extra cooling, are hard to confirm. It is possible that the rapid recombination occurs following some other electron cooling process, or even by means of a mechanism other than that of the three-body collisional recombination described here. For this reason, the predictions of the model for the temperature of the cold electron class may not be entirely reliable. The inclusion of the "extra cooling," due to the Ne($2p^5 3s$)

population buildup, in the model results in very good agreement of the model with experimental observations of populations in a variety of atomic and ionic levels. It seems very likely that some such extra cooling is indeed present. Further work is required, however, to verify the existence of the $Ne(2p^5 3s)$ population buildup or, alternatively, to identify other possible sources of extra electron cooling or different mechanisms of electron recombination.

The possibility of creating conditions where such rapid recombination can occur may be of considerable importance for the further development of lasers based on recombination processes[11,12] and may allow the extension of recombination laser action to shorter wavelengths. In such laser systems, a poplation inversion is produced when the rate into the upper laser level by recombination is large compared to the deexcitation rate of that level by spontaneous emission or by electron deexcitation. At the same time, the lower laser level must remain relatively empty. For short wavelength lasers, the radiative emission rate from the upper to lower laser level becomes large, since that rate is inversely proportional to the square of the emission wavelength. For example, for an oscillator strength of $f = 0.1$, at a wavelength of 100 nm, the radiative decay rate is 7×10^8 s^{-1}. Thus the recombination rates observed in this work (in excess of 10^9 s^{-1}), together with the large densities (10^{15}–10^{16} cm^{-3}) of electrons and ions available to participate in the production of the upper laser level by recombination, suggest that the PES could be very suitable as an excitation technique for the production of short wavelength recombination lasers.

In addition to the rapid recombination that can be observed, a PES-excited plasma, such as the Li-Ne mixture studied here, exhibits two important properties. The PES excitation creates a population distribution among the "target" alkali-metal atoms (in this case Li) in which the atoms are equally distributed between the ground state and the first excited level [$Li(1s^2 2p)$]. This distribution is maintained for a period of more than 10 ns. At the same time, the electron and alkali-metal ion densities are more than an order of magnitude lower (Fig. 5).

The extremely nonequilibrium nature of the population distribution, in the Li-Ne mixture discussed here, could lead to a number of interesting applications for this type of PES excitation. The production of large densities (7×10^{16} cm^{-3}) of excited atoms is important for spectroscopic applications as it allows the observation of transitions to atomic levels of the same parity as the atomic ground state. Another potential use of a large density of excited atoms is to act as a medium for nonlinear optical interactions, such as the Raman shifting of available laser sources to new wavelengths.

A third area in which PES excitation could have a significant impact is for the excitation of laser systems requiring the types of population distributions produced by the PES. Some examples of these are the various metal–noble-gas excimer laser systems[5–7] and radiative-collision lasers.[4] One of the most promising of the former laser systems is the Li-Xe system. This mixture can be expected to behave (under PES excitation) in a qualitatively similar manner to that of the Li-Ne mixture discussed

here. In order for net gain to be observed for the Li-Xe excimer laser system, it is necessary for the $Li^*(2p)$ level density to exceed 5% of the $Li(2s)$ ground-state density[5]—a condition that can easily be realized in a PES-excited plasma. To significantly shift the Li resonance line emission to the Li-Xe molecular A-X band, densities of Xe in excess of 10^{20} cm^{-3} are required. It seems reasonable to assume that comparable Li population distributions to those reported here could be achieved at such high Xe densities. In that case, it appears that PES excitation of such a Li-Xe system could lead to gains as high as 100 m^{-1} on the A-X band of the Li-Xe molecule at wavelengths around 900 nm. Similar systems, such as the A-X band of Na-Xe, should also be readily excited by the PES.

The class of radiative-collisional lasers, proposed by Harris, Falcone, and O'Brien,[4] seems similarly suited to excitation by the PES. Again, laser emission requires high densities of resonance level alkali-metal atoms. For a vapor of Rb, with a density of 5×10^{16} cm^{-3} atoms excited to the $Rb(4p^6 5p)^2 P_{3/2}$ level, a gain of 8% cm^{-1} is predicted[4] at 5.4 μm. Such a population distribution seems readily achievable with the PES and it should be possible to perform the first demonstration of this class of laser using PES excitation.

It should be noted that the production of high densities of alkali-metal resonance level atoms, and of nonequilibrium population distributions similar to those that are reported here, has been demonstrated by McIlrath and Lucatorto.[8,9] In that work, the excitation technique that was used was photoexcitation of the atomic resonance level by means of high-power laser radiation. The dynamics of that interaction, which results in complete ionization of the atomic system at later times, has been extensively studied by various authors.[28–30] In many respects, excitation by the PES is complementary to the photoexcitation technique. It extends the range of accessible transitions from those which can be excited by laser pumping to include both dipole-allowed and dipole-forbidden transitions of all energies up to approximately 100 eV. Also, because the PES excitation emanates from a laser-produced plasma inside the vapor, resonance level saturation can be achieved in high-density atomic vapor without the requirement of a high-energy laser to "burn through" a column of high-density vapor.

VII. SUMMARY

The photoionization electron source is a new technique by which high densities of hot electrons can be supplied to excite an atomic vapor. From Fig. 5 it can be seen that, at its peak, the hot electron density at a distance of 1 mm from the x-ray-producing plasma is in excess of 5×10^{15} cm^{-3}. Under these conditions, the hot electron distribution has a temperature of 15 eV. This corresponds to a peak current density of 2×10^5 A cm^{-2} and far exceeds that achievable by conventional discharge excitation.

The high temperature of the electrons which it produces makes the PES ideally suited for the excitation of highly energetic atomic and ionic levels. This was well illustrated in the first demonstration of the PES in which

Li($1s\,2s\,2p$)$^4P^0$ levels at 57.4 eV were excited in densities roughly 3 orders of magnitude larger than had been previously achieved with conventional fast discharge technology.[31] As well as exciting high-energy levels, the PES is capable of producing very high densities of lower-energy excited levels such as the Li($1s^2 2p$) resonance level. Because of the short duration of the PES excitation, very nonequilibrium population distributions can be achieved and excitation rates can equal or exceed typical extreme-ultraviolet radiative decay rates of 10^{10}–10^{11} s^{-1}. These properties suggest a number of possible applications for PES excitation, ranging from the preparation of atomic media for spectroscopy and nonliner optics to the use as an excitation technique for xuv three- and four-level laser systems.

In this work, a detailed experimental and theoretical investigation has been presented of the population distribution in a Li-Ne vapor excited by the PES. The expected high densities of excited levels and nonequilibrium population distributions have been observed and the agreement of theory and experiment is seen to be good. An excep-

tionally rapid recombination rate is the key to an understanding of the development of the excited-state populations. This rapid recombination can be completely described by the conventional theory of three-body collisional recombination [Eqs. (16) and (17)], providing electron temperatures of the order of 0.1 eV are reached in the cold electron class. In this case, the unusual rapidity of the recombination is a result of the large electron density (10^{15}–10^{16} cm^{-3}) and the low electron temperature in the PES-excited vapor. The details of the mechanism for achieving such low temperatures require confirmation.

ACKNOWLEDGMENTS

*Present address: Stanford Research Systems, Inc., 460 California Avenue, Palo Alto, CA 94306.

[1]J. C. Wang, R. G. Caro, and S.E. Harris, Phys. Rev. Lett. 51, 767 (1983).

[2]S. E. Harris, Opt. Lett. 5, 1 (1980).

[3]J. E. Rothenberg and S. E. Harris, IEEE J. Quantum Electron. QE-17, 418 (1981).

[4]S. E. Harris, R. W. Falcone, and D. M. O'Brien, Opt. Lett. 7, 397 (1982).

[5]A. Gallagher, in Excimer Lasers, Vol. 30 of Topics in Applied Physics, edited by C. K. Rhodes (Springer, New York, 1979).

[6]R. Shuker, A. Gallagher, and A. V. Phelps, J. Appl. Phys. 51, 1306 (1980).

[7]L. A. Schlie, J. Appl. Phys. 47, 1397 (1976).

[8]T. B. Lucatorto and T. J. McIlrath, Phys. Rev. Lett. 37, 428 (1976).

[9]T. J. McIlrath and T. B. Lucatorto, Phys. Rev. Lett. 38, 1390 (1977).

[10]N. M. Ceglio, R. L. Kauffman, A. M. Hawryluk, and H. Medecki, Appl. Opt. 22, 318 (1983).

[11]W. T. Silfvast and O. R. Wood II, in Laser Techniques for Extreme Ultraviolet Spectroscopy (Boulder, 1982), edited by T. J. McIlrath and R. R. Freeman (AIP, New York, 1982), Vol. 90, p. 128.

[12]W. T. Silfvast and O. R. Wood II, Opt. Lett. 8, 169 (1983).

[13]R. G. Caro, J. C. Wang, R. W. Falcone, J. F. Young, and S. E. Harris, Appl. Phys. Lett. 42, 9 (1983).

[14]R. G. Caro, J. C. Wang, J. F. Young, and S. E. Harris, Phys. Rev. A 30, 1407 (1984).

[15]S. S. Penner and R. W. Kavanagh, J. Opt. Soc. Am. 43, 385 (1953).

[16]D. S. Rozhdestvenskii, Ann. Phys. (Leipzig) 39, 307 (1912).

[17]W. C. Marlow, Appl. Opt. 6, 1715 (1967).

[18]A. B. Duval and A. I. McIntosh, J. Phys. D 13, 1617 (1980).

[19]H. R. Griem, Spectral Line Broadening by Plasmas (Academic, New York, 1974).

[20]W. R. Hindmarsh and J. M. Farr, in Progress in Quantum Electronics, edited by J. H. Sanders and S. Stenholm (Pergamon, New York, 1972), Vol. 2, Part 3.

[21]L. Spitzer, Jr., in Physics of Fully Ionized Gases, Vol. 3 of Interscience Tracts on Physics and Astronomy, edited by R. E. Marshak (Interscience, New York, 1956).

[22]H. van Regemorter, Astrophys. J. 136, 906 (1962).

[23]M. Gryzinski, Phys. Rev. 138, A336 (1965).

[24]H. W. Drawin and F. Emard, Physica 85C, 333 (1977).

[25]E. Hinnov and J. G. Hirschberg, Phys. Rev. 125, 795 (1962).

[26]H. W. Drawin and P. Felenbok, Data for Plasmas in Local Thermodynamic Equilibrium (Gauthier-Villars, Paris, 1965).

[27]H. A. Hyman and S. A. Mani, Opt. Commun. 20, 209 (1977).

[28]T. B. Lucatorto and T. J. McIlrath, Appl. Opt. 19, 3948 (1980).

[29]R. M. Measures, N. Drewell, and P. Cardinal, J. Appl. Phys. 50, 2662 (1979).

[30]B. Carré, F. Roussel, P. Breger, and G. Spiess, J. Phys. B 14, 4271 (1981); 14, 4289 (1981).

[31]D. E. Holmgren, R. W. Falcone, D. J. Walker, and S. E. Harris, Opt. Lett. 9, 85 (1984).